TRANSIENT CHF PHENOMENA DUE TO EXPONENTIALLY INCREASING HEAT INPUTS

JONGDOC PARK*, KATSUYA FUKUDA[1] and QIUSHENG LIU
Oshima National College of Maritime Technology
1091-1, Komatsu, Suo-Oshima-cho, Oshima-gun, Yamaguchi, 742-2106, Japan
[1] Kobe University, Graduate School of Maritime Sciences
5-1-1, Fukueminami, Higashinada, Kobe, 658-0022, Japan
*Corresponding author. E-mail : park@oshima-k.ac.jp

Received January 6, 2009
Accepted September 4, 2009

The critical heat flux (CHF) levels that occurred due to exponential heat inputs for varying periods to a 1.0-mm diameter horizontal cylinder immersed in various liquids were measured to develop an extended database on the effect of high subcoolings for quasi-steady-state and transient maximum heat fluxes. Two main mechanisms of CHF were found. One mechanism is due to the time lag of the hydrodynamic instability (HI) which starts at steady-state CHF upon fully developed nucleate boiling, and the other mechanism is due to the explosive process of heterogeneous spontaneous nucleation (HSN) which occurs at a certain HSN superheat in originally flooded cavities on the cylinder surface. Steady-state CHFs were divided into three regions for lower, intermediate and higher subcooling at pressures resulting from HI, transition and HSN, respectively. HSN consistently occurred in the transient boiling CHF conditions that correspond to a short period. It was also found that the transient boiling CHFs gradually increased, then rapidly decreased and finally increased again as the period became shorter.

KEYWORDS : Transient Boiling, Pool Boiling, CHF, Exponential Heat Input

1. INTRODUCTION

There is a class of severe, design-based accidents that may occur in a water-cooled nuclear power reactor due to surges in the power produced by the reactor. To predict the likelihood of such accidents, it is necessary to understand the transient boiling phenomenon that accompanies such power surges and that is caused by increasing heat inputs in subcooled water at high pressures. Research into generalized pool boiling critical heat flux (CHF) mechanisms and their correlations in water (as a non-wetting liquid) and wetting liquids such as ethanol, liquid nitrogen, liquid helium and Fluorinert (FC liquids) is becoming increasingly important for the development of a database of basic information on the following problems: (a) the safety assessment of severe nuclear reactor accidents such as power bursts, rapid depressurization and vapor explosions in the reactor; (b) meeting the recent need for the design of stable, high-heat flux cooling systems; and, (c) the derivation of subcooled flow boiling CHF correlations based on pool boiling CHF correlations. Many aspects of saturated and subcooled pool boiling CHFs in liquids have been investigated by various researchers, including pressure, subcooling, test heater configurations, surface roughness, and thermal properties, etc., assuming a CHF model based mainly on a kind of hydrodynamic instability (HI) in the CHF that was first suggested by Kutateladze [1] and Zuber [2]. A few key aspects of the complex CHF phenomena are as yet not fully understood.

This study addresses the role of the form of spontaneous nucleation called heterogeneous spontaneous nucleation (HSN) that occurs in the originally flooded cavities on the surface of a cylinder. The HSN phenomenon occurs when a new phase appears at an interface or a boundary rather than in the bulk fluid, similarly to the phenomenon of homogeneous spontaneous nucleation [3]. It has been clarified by Sakurai et al. [4] that CHFs due to steady and transient heat generation rates on the cylinder surface at certain conditions in water are determined by the explosive process of heterogeneous spontaneous nucleation (HSN). The HSN phenomenon occurs at the HSN surface superheat in originally flooded cavities on the cylinder surface. It has been observed on the cylinder surface in previously degassed water under a high pressure of 5 MPa before each experimental run. The initiation of boiling that occurred from active cavities previously entraining vapor was replaced by boiling initiated by the HSN in originally flooded cavities. Even for the case where the pre-pressure process was not applied, the critical heat flux due to HSN in the fully developed nucleation regime caused by a

steadily increasing heat input was observed for the first time for a pool of highly subcooled water under high pressure conditions. It was found that CHF was significantly lower than the value derived from the CHF correlation obtained based on HI [5,6]. The direct transition from a non-boiling regime such as a natural convection or transient conduction regime to film boiling without nucleate boiling was observed by Sakurai et al. as having occurred due to HSN in a pool of wetting liquids and pre-pressurized water [4,6]. Such a direct transition was reported by Avksentyuk & Mamontova [7] and Kutateladze et al. [8] in liquid metals and wetting liquids as a peculiarity of the CHF process. However, the mechanism of CHFs for transient heat inputs with shorter periods has remained unresolved for a long time. Sakurai et al. have provided a detailed clarification of the effect of HSN on the mechanism of CHFs for transient heat inputs. They assumed that the transitions occurred due to the levitation of liquid on the cylinder surface by the explosive HSN process in originally flooded cavities without the contribution of the active cavities through entraining vapors to cause boiling.

Typically, measured CHF values have been classified into three groups depending on long, intermediate, and short periods. The CHF gradually increased to a maximum value from a steady-state CHF, and then the CHF quickly decreased to a minimum value; finally, the CHF again increased, accompanied by a decrease in period. The steady-state CHF corresponds to the CHF due to the heat input with a period τ of 20 s. This anomalous CHF trend has been reported in previous studies at various pressures for low subcoolings [9-11]. It was clarified that there are two main mechanisms of CHF depending on the time period that corresponds to exponential heat generation rates.

As a continuation of previous work [9-11], steady state and transient boiling CHFs in pools of liquid were studied in this paper. Boiling heat transfer processes on a horizontal cylinder in water (which was the non-wetting liquid used here) or highly wetting liquids due to exponentially increasing heat inputs with various periods were measured for a wide range of subcoolings and pressures to get an extended database of the effects of high subcoolings. The objectives of this work are to clarify the effects of various pressures, subcoolings and periods for a pool boiling CHF, and to clarify the generalized CHF phenomena that occur at a steady and transient CHF according to the wettability of boiling liquids.

2. EXPERIMENT APPARATUS AND METHOD

2.1 Pool Boiling Apparatus

The experimental apparatus is shown in Fig. 1. It consists of a boiling vessel, an experimental heater shaped in a horizontal cylinder, a pressurizer, a device to control the heat generation rate, a data measurement and processing system, and a high-speed video camera. The boiling vessel has inspection windows and is made of stainless steel; it has an inner diameter of 200 mm and a height of 600 mm. The experimental heater is a 1.0-mm diameter cylinder which is horizontally immersed in the vessel. The diameter was determined after the diameter dependency reported by Lienhard et al. [12] that shows a prediction curve for cylinders. As shown in the curve, the non-dimensional length L' ($= (D/2)\sqrt{g(\rho_l - \rho_v)/\sigma}$) becomes the diameter that is considered to be Zuber's infinite horizontal flat plate. The effective length of the heater between the potential taps is about 31 mm.

2.2 Experimental Method and Procedure

The cylinder is heated electrically by a direct current source controlled by a computer as the current is increased in an exponential function with time. The analog computer computes the instantaneous mean temperature of the

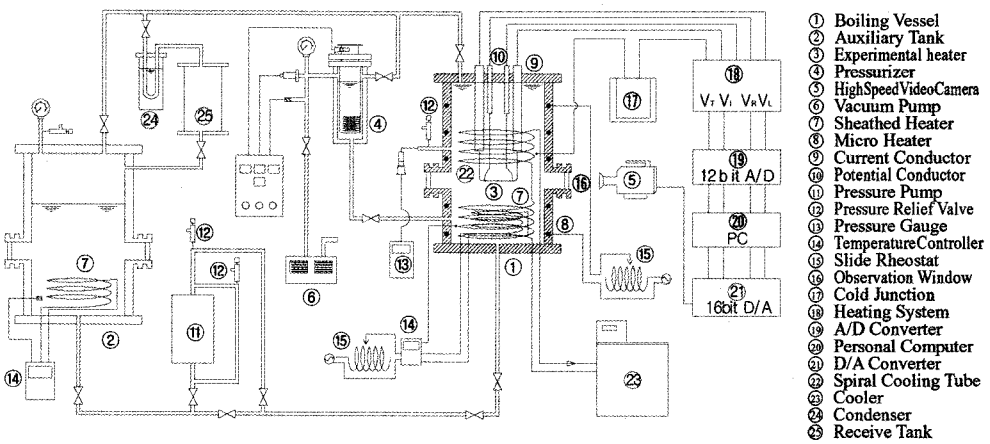

Fig. 1. Schematic Diagram of Experimental Apparatus

Table 1. Experimental Condition

Parameter	Condition
Cylinder	platinum wire
Liquid	water, ethanol, FC-72
Pressure	101.3-1572 kPa
Subcooling	0-160 K
Period	0.005 s-50 s

cylinder and it cuts off the power supply when the calculated mean temperature reaches a preset value by using a burnout detector. The output voltages of the double bridge circuit, together with the voltage drops across the potential taps of the cylinder and across a standard resistance, were amplified and passed through analog-to-digital (A/D) converters installed in the computer. These voltages were simultaneously sampled at a constant time interval that was changed depending on the period. The fastest sampling speed of the A/D converter is 5μs/channel. The average temperature between the potential taps was measured by resistance thermometry using the cylinder itself. The heat generation rate was determined from the current to the cylinder and the voltage difference between potential taps on the cylinder. The surface temperature was obtained by solving the conduction equation in the cylinder under the conditions of the average temperature and heat generation rate. The CHF was determined at a start point where the average temperature rapidly increases up to the preset temperature by using a burnout detector that is lower than the actual burnout temperature of a platinum wire. The uncertainties are estimated to be within ±1 percent for the heat generation rate, ±2 percent for the heat flux and to be within ±1 K for the cylinder surface temperature.

The heat generation rate Q was raised with an exponential function as follows:

$$Q = Q_0 \exp(t/\tau) \tag{1}$$

where Q_0 is initial heat generation rate, t is time, and τ is period. Period τ is an e-fold time that corresponds to exponential heat generation rate. The exponential period τ of the heat input ranged from quasi-steadily increasing heat inputs to rapidly increasing ones. The heat flux q was calculated by the following equation for heat balance.

$$q = \frac{D}{4} Q - \rho_h c_h \frac{D}{4} \frac{dT_a}{dt} \tag{2}$$

where D, ρ_h, c_h and T_a are the diameter, density, specific heat and the average temperature of the cylinder, respectively. The surface temperature can be calculated from the unsteady heat conduction equation of the next expression by assuming the surface temperature around the test heater to be uniform.

$$\frac{\partial T}{\partial t} = a\left[\frac{\partial^2 T}{\partial r^2} + \frac{1}{r}\frac{\partial T}{\partial r}\right] + \frac{Q}{\rho c} \tag{3}$$

Boundary conditions are as follows:

$$\left.\frac{\partial T}{\partial t}\right|_{r=0} = 0, \quad -\lambda \left.\frac{\partial T}{\partial r}\right|_{r=R} = q$$

$$T_a = \frac{\int_0^R T(2\pi r)dr}{\int_0^R (2\pi r)dr} = \frac{2}{R^2}\int_0^R Tr dr$$

where Q [W/m^3] is the internal heat generation rate, T [K] is the temperature inside the cylinder, $a = k/\rho c$ [m^2/s] is the thermal diffusivity, and k [W/mK] is the thermal conductivity.

The experiment was carried out as follows. First, the experimental liquids were degassed by keeping them boiling for at least 30 minutes in the auxiliary tank. Vapor was recovered to the pool with a water-cooled condenser. The liquid was fully filled in the boiling vessel with the free surface only in the pressurizer and sub tank. Liquid temperatures in the boiling vessel and in the pressurizer were separately controlled to realize the desired saturated and subcooled conditions. Each heat flux and surface superheat was calculated by the data processing system according to time.

2.3 Boiling Heat Transfer Process in Ethanol

Figure 2 shows typical changes in the cylinder wall temperature, T_w, and heat flux, q, with time for an exponential heat generation rate, Q, with a period of 1.45 s at a pressure of 494 kPa under saturated conditions in ethanol. The heat generation rate, Q, increases exponentially regardless of the changes in surface temperature. The heat flux, q, increases with an increase in Q. After the point when boiling begins, q_{in}, the heat flux shows a rapid overheating and decrease regime caused by a bump of vapor bubbles and liquid flow on the cylinder surface. The q increases again exponentially to reach the critical heat flux point, q_{cr} (=CHF). T_w also increases with an increase in Q. T_w continues to increase up to T_{ov} (called the overshot point), then rapidly decreases before increasing once again, this time at a low rate. When q reaches CHF, T_w rapidly increases with time.

Figure 3 shows the typical boiling curve on a graph of log q versus log ΔT_{sat} for the experimental run shown in Fig. 2. The surface superheat ΔT_{sat} is defined by the difference between the surface temperature of the cylinder and the saturation temperature of liquid corresponding to the experimental pressure. As shown in the figure, heat flux, q, increases at a rate slightly above the natural convection curve [15] in a non-boiling regime. After q_{in}, the initiation of boiling, the surface superheat rapidly

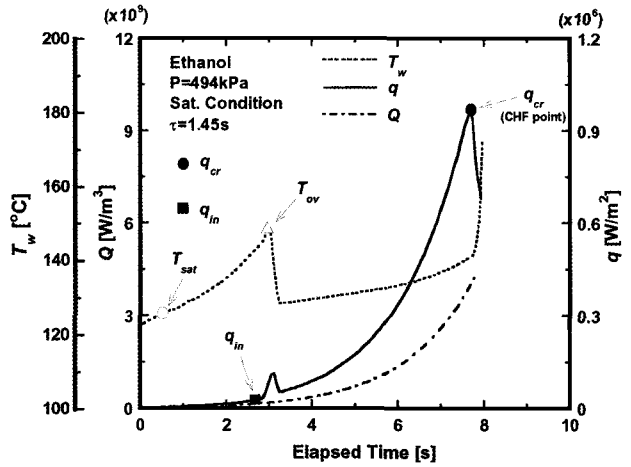

Fig. 2. Illustrative Time Traces of Heat Generation Rate, Q, Cylinder Wall Temperature, T_w and Heat Flux, q

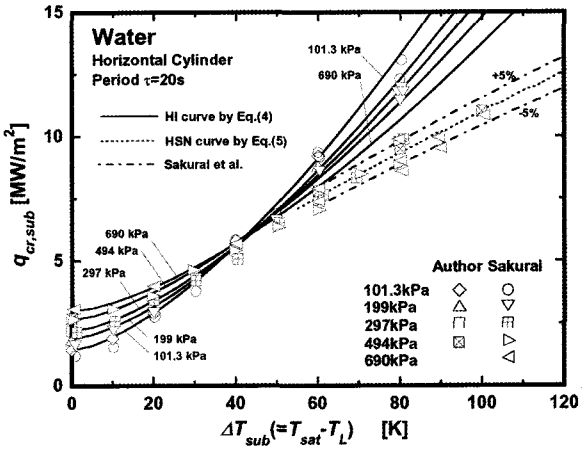

Fig. 4. Comparison of Prediction with $q_{cr,sub}$ for Subcooling with Pressures as a Parameter in Water using Eqs.(4), (5) and Sakurai's Data

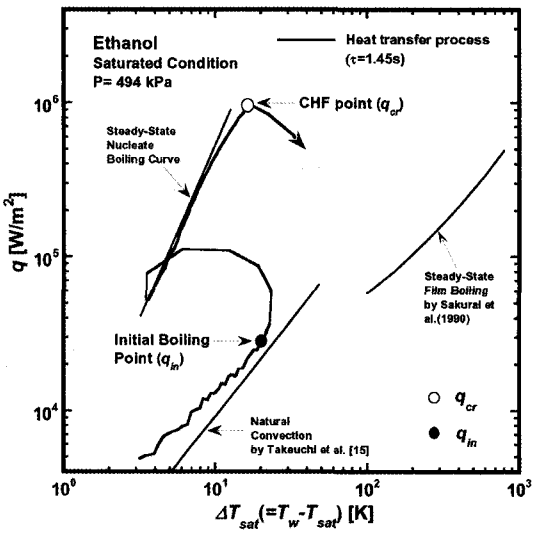

Fig. 3. Boiling Heat Transfer Process from Non-boiling to Fully-developed Nucleate Boiling

decreases, and q increases along the fully-developed nucleate boiling (FDNB) regime and reaches the CHF point, q_{cr}. At that point, the transition to film boiling occurs.

The boiling process is expected to be changed depending on the exponential period of heat input. It is considered that the different types of boiling curve can be shown in cases with periods much shorter than 1.45 s.

3. EXPERIMENTAL RESULTS & DISCUSSION

3.1 Steady-state CHFs for a Wide Range of Subcoolings and Pressures in Water

In this study, heat transfer processes for periods longer than 10 s are considered as quasi-steady-state processes, because the non-boiling region in such processes agrees well with the natural convection curve, and all CHFs measured for the heat inputs with periods longer than 10 s are almost the same. We measured the CHFs on a horizontal cylinder in water for various pressures and subcoolings that occurred due to quasi-steadily increasing heat input according to exponential time function. The obtained $q_{cr,sub}$ values are shown in Fig. 4 for subcoolings with pressure as a parameter. The subcooling ΔT_{sub} is defined by the difference between the saturation temperature of the liquid, which corresponds to the experimental pressure, and the liquid temperature of each experiment.

The following correlation was derived by modifying Kutateladze's correlation while taking into account the non-linear effect of high liquid subcoolings on the q_{cr}.

$$q_{cr,sub} = q_{cr,sat}\left[1 + K_2(\rho_l/\rho_v)^{0.69}(C_{pl}\Delta T_{sub}/L_H)^{1.5}\right], \quad \text{HI curve} \qquad (4)$$

where $q_{cr,sat} = K_1 L_H \rho_v [\sigma g(\rho_l - \rho_v)/\rho_v^2]^{0.25}$ given by the Kutateladze correlation. K_1 values are almost 0.17 independent of the cylinder diameters, and K_2=0.40$(L')^{-0.6}$.

The power value of 1.5 in Eq. (4) was determined, so that Eq. (4) can better express the experimental data for subcoolings. The values of CHF predicted by Eq. (4) and Sakurai's data [5] are shown in comparison with our experimental data in the figure. Almost all of the $q_{cr,sub}$ data versus subcoolings with pressures as a parameter agree well with the correlations given by Kutateladze [1] based on the model of CHF resulting from HI.

However, a large number of the $q_{cr,sub}$ values measured for highly subcooled water at high pressure cannot be expressed by Eq. (4). For cases with pressures higher than

400 kPa, most of the data does not agree with the values derived from Eq. (4) when subcoolings become higher than 60 K. Sakurai et al. conducted an experiment on the same cylinder in water for a wider range of subcoolings and pressures, and they derived the empirical equation of CHF for high subcoolings at high pressures.

$$q_{cr,sub} = K_3 \Delta T_{sub}^{0.73}, \quad \text{HSN curve for water} \qquad (5)$$

The curve given by Eq. (5) is also shown in Fig. 4. The measured $q_{cr,sub}$ ranged within ±5% of the $q_{cr,sub}$ curve for subcooling, as derived from Eq. (5) with the K_3 value of 3.81×10^5. The $q_{cr,sub}$ values for this range are almost independent of pressure. It was previously assumed that the heat transfer crisis at the CHFs expressed by Eq. (5) occurred due to heterogeneous spontaneous nucleation, HSN, in originally flooded cavities on the cylinder surface when liquid was present.

Consequently, it is clarified that the CHFs measured can be classified into two mechanisms for lower and higher subcooling at various pressures in water. One mechanism is dependent on the HI, and the other mechanism is dependent on the HSN. The CHFs that occurred due to the HSN for high subcoolings at high pressures are significantly lower than the CHF correlation obtained based on the HI. This difference in CHFs is important to recognize for the safety assessment of severe nuclear reactor accidents and the cooling stability design of high heat flux cooling systems.

3.2 Typical Heat Transfer Processes with and without Pre-pressurization in Water

As described above, it was confirmed that the transition at CHF on the cylinder surface at high pressure for highly subcooled water was determined by the explosive process of heterogeneous spontaneous nucleation (HSN). The HSN phenomenon was observed on the cylinder surface in previously degassed water before each experimental run through a process of pre-pressurization to 5 MPa.

On a graph of heat flux q versus surface superheat ΔT_{sat}, Fig. 5 shows the heat transfer processes with and without pre-pressurization in response to the exponential heat inputs for the period of 20 s (this refers to the quasi-steadily increasing heat input) at a pressure of 494 kPa for a subcooling of 60K in water. The heater used in Sakurai's experiment [5] was a horizontal cylinder of pure platinum, as was used in this present study. Both cylinders are commercially-available products with no surface preparation, so it is assumed that there is no difference between the surface roughness of the two cylinders. It is worth noting the effect of pre-pressurization here. It can be found that the processes of boiling initiation show completely different according to the level of pre-pressurization. The CHF values are almost the same regardless of pre-pressurization, and the processes up to CHF points in a fully developed nucleate boiling (FDNB) regime almost agree with each other. In terms of the experimental conditions for high subcooling at high pressure, the values of CHF that result from HSN are expressed by Eq. (5).

The typical heat transfer process of the case without pre-pressurization is shown with a dashed line: heat flux, q, gradually increases along the natural convection curve [15] at first, and after the incipience of boiling at a surface superheat of around 3.5 K (mark ● ΔT_{in}), the heat flux, q, rapidly increases with an increase in surface superheat up to the FDNB regime, then reaches the CHF point, q_{cr}. In this case, it is assumed that the incipience of boiling is from numerous active cavities entraining vapor that cause the rapid increase of heat flux.

The HSN mentioned here occurs at a certain HSN superheat that is significantly lower than the superheat of an HSN on a smooth flat solid surface, and lower than the homogeneous spontaneous nucleation temperature in liquid. The occurrence of HSN in water due to a quasi-steadily increasing heat input was observed at a certain superheat temperature, ΔT_{in}, in the case with pre-pressurization. The temperature is referred to here as ΔT_{inLH}, and is the lower limit of HSN superheat (mark ▲). The values in water, LHe I, N_2 and ethanol have already been observed and presented by Sakurai et al. [4]. As shown in the figure, the surface superheat ΔT_{cr} at the CHF point almost agrees with the ΔT_{inLH} value. It is assumed that the heat transfer crisis at CHF for high subcoolings at high pressures occurs at a ΔT_{inLH} point in the FDNB regime due to the explosive process of HSN in originally flooded cavities on the cylinder surface.

Figure 6 shows the heat transfer processes with and without pre-pressurization for the period of 0.01 s (indicating a rapidly increasing heat input) in saturated

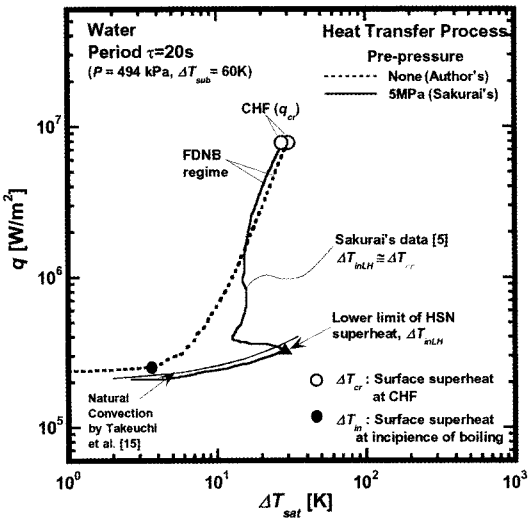

Fig. 5. Typical Heat Transfer Processes with and without Pre-pressurization for Period of 20 s in Water

water at atmospheric pressure. For boiling processes with shorter periods, the direct or semi-direct transition to film boiling occurs with an explosive transition from non-boiling to boiling.

In the case of pre-pressurized water, indicated in the figure with a solid line, the CHF point (marked with the symbol ●) is due to the direct transition from a single-phase conduction regime to film boiling; the value ΔT_{in} is equal to ΔT_{cr}. It is considered that the direct boiling transitions occur due to the levitation of liquid on the cylinder surface caused by the explosive HSN in originally flooded cavities, without the contribution of the entraining vapors of the active cavities. The heat transfer process of the case without pre-pressurization is shown with a dashed line. After the incipience of boiling, the heat flux, q, slightly increases with insufficient nucleate boiling. That is why the incipience of boiling on the cylinder surface causes an increasing heat input from originally unflooded active cavities that entrain vapor bubbles.

The CHFs with transition process can be classified into three principal groups according to period τ. In the first group CHFs, the CHF occurred through a fully developed nucleate boiling (FDNB), as shown in Fig. 5, and the CHF usually occurred for longer period. In the second group CHFs, shown in Fig. 6, shorter period were used, and there was a direct transition to film boiling without nucleate boiling. The third group CHFs had an intermediate period between those of the first and second groups.

3.3 Typical Transition to Film Boiling at q_{cr} for τ in Water and Ethanol

There are two types of boiling incipience on the cylinder surface in a liquid due to an increasing heat input; one occurs as a result of numerous active cavities entraining vapor and the other acts by a different mechanism that does not require the contribution of the active cavities. The former is observed in water. The latter occurs in highly wetting liquids such as ethanol, FC-72, and liquid nitrogen, and in water that is sufficiently pre-pressurized. The latter boiling mechanism was suggested by Sakurai et al. [4] to be due to the HSN from originally flooded cavities on the cylinder surface in such liquids.

Figure 7 shows transient CHFs, q_{cr}, and incipient boiling heat fluxes, q_{in}, versus periods, τ, ranging from 0.005 s to 20 s in saturated water at atmospheric pressure, in the cases without and with pre-pressurization (cases 1 and 2, respectively). The values for case 2 are from Sakurai's data [6]. As shown in the figure, the q_{cr} values for cases 1 and 2 increase, then decrease and again increase with a decrease in period. The values are classified into three groups that correspond to the cases, although the q_{cr} values in the second group for case 1 and the q_{cr} values in the third group for case 2 were not observed.

The q_{cr} for case 2 changes to that of the second group for periods shorter than around 2 s. This means that direct transition from a non-boiling regime to film boiling occurs in periods of rapid heat increase, as shown in Fig. 6. The q_{in} values in the second group are equal to q_{cr}. It should be noted that the direct transitions occur over a remarkably large range in period when using pre-pressurized water. On the other hand, the second group of q_{cr} for case 1 without pre-pressurization was not tested here, but it can be supposed that direct transitions occur for periods shorter than about 0.005 s. In this case, the third group of q_{cr} is clearly present, as shown in Fig. 7. The q_{cr} decreases with the decrease in period from the maximum q_{cr} to the minimum q_{cr}. It was assumed that the heat transfer crisis at q_{cr} in the third group occurs due to the HSN in originally flooded cavities on a solid surface. HSN is believed to have occurred under conditions of insufficiently developed

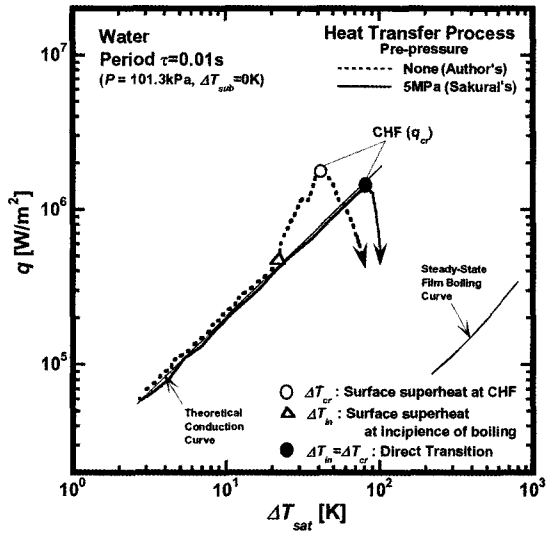

Fig. 6. Typical Heat Transfer Processes with and without Pre-pressurization for Period of 0.01 s in Water

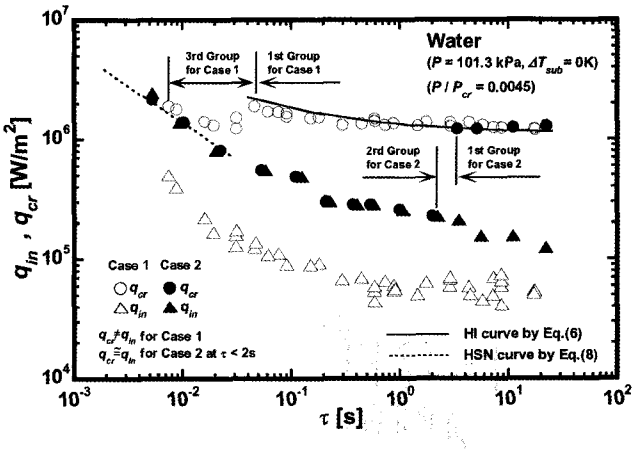

Fig. 7. Incipient Boiling Heat Flux, q_{in}, Critical Heat Flux, q_{cr} vs. Period, τ, for Saturated Water at Atmospheric Pressure

nucleate boiling at the surface superheat of around the lower limit of HSN temperature as a result of the accompanying gradual increase in the surface superheat.

By the effect of pre-pressurization, the boiling initiation mechanism was changed from that of active cavities entraining vapor to that of the HSN in originally flooded cavities for the periods between 0.005 s and 2 s. This means that the CHF characteristic for pre-pressurized water becomes similar to that of highly wetting liquids such as ethanol and FC-72.

On the other hand, as shown in Fig. 8, it could be easier for the highly wetting liquid ethanol than for water to flood cavities on the cylinder surface because it has a lower surface tension than water and the value of the liquid-solid contact angle on the cylinder surface is smaller than that of water. Although the CHF values in the figure are for the case without pre-pressurization, it was found that the direct transitions belonging to the second group CHF (q_{cr}) occur with remarkable frequency. This means that the CHF characteristic is similar to that from the pre-pressured water, as shown in Fig. 7. The CHF belonging to the first group slightly increases from a steady-state CHF, then suddenly decreases to a minimum CHF belonging to the second group and finally increases again with the decrease of period. It is considered that the direct boiling transition from non-boiling to film boiling is due to HSN, as mentioned before.

Fukuda et al. [13] suggested the several empirical equations that are used here for a wide range of subcoolings and pressures to represent the transient CHF values versus periods belonging to the first and second groups. The CHFs belonging to the first group and caused by the heat generation rates with a long period under a saturated condition are expressed by Eq. (6) and those developed under a high subcooled condition are expressed by Eq. (7). The CHF belonging to the second group with a short period is expressed by Eq. (8).

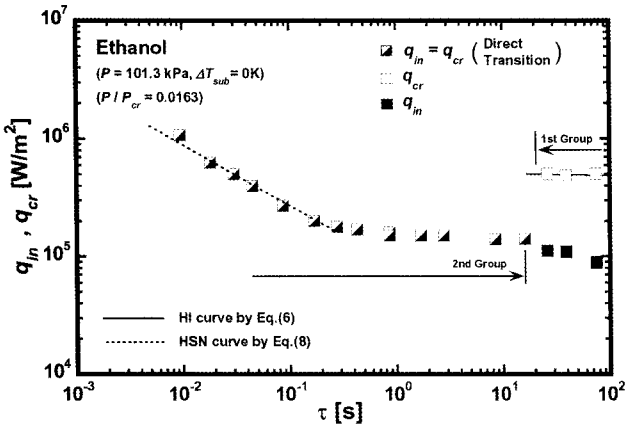

Fig. 8. Boiling Initiation Heat Flux, q_{in}, Critical Heat Flux, q_{cr} vs. Period, τ, for Saturated Ethanol at Atmospheric Pressure

$$q_{cr} = q_{st,sub}\left(1 + 0.21\tau^{-0.5}\right),$$
1st group for saturated condition (due to HI) (6)

$$q_{cr} = q_{st,sub}\left(1 + 2.3\times10^{-2}\tau^{-0.7}\right),$$
1st group for high subcooled one (due to HSN) (7)

where $q_{st,sub}$ is given by the quasi-steady-state CHF data in each experiment.

$$q_{cr} = h_c\left(\Delta T_{in}(\tau) + \Delta T_{sub}\right),$$
2nd group (due to HSN) (8)

where $h_c \cong (k_l/\rho_l c_{pl}/\tau)^{1/2}$. The symbol of h_c is the heat transfer coefficient resulting from transient heat conduction. $\Delta T_{in}(\tau)$ is the surface superheat at incipience of boiling due to the HSN in the conduction regime, and the $\Delta T_{in}(\tau)$ was measured for periods at every experimental condition. The surface superheat at boiling initiation depends on the increasing rate of period, pressure and liquid subcooling [5,13].

As mentioned in section 3.2, the CHF belonging to the 1st group with a longer period occurs with a FDNB heat transfer process. The steady-state CHFs were due to either HI or HSN, depending on the experimental conditions. For the 2nd group with shorter periods, the direct transition to film boiling from non-boiling occurs as an explosive boiling. It is considered that the direct transition process expressed by Eq. (8) is due to HSN at the incipience of boiling. On the other hand, as confirmed in the steady-state CHF in Fig. 4, for high subcoolings at high pressures, the $q_{cr,sub}$ values resulted from the HSN, and the $q_{cr,sub}$ values were significantly lower than those expected by the correlation based on HI. Therefore, as regards Eq. (7), it is assumed that the trend of the CHFs for the various periods becomes different from the corresponding curve estimated by Eq. (6). This will be described in more detail later.

3.4 Steady-state CHFs in Wetting Liquids such as Ethanol and FC-72

Figure 9 shows steady-state CHF data for subcoolings up to 160 K over pressures from 297 kPa to 1572 kPa in a pool of ethanol with corresponding CHF curves obtained by empirical equations from [14], and Fig. 9 also shows calculations made using Eqs. (4) and (9) for comparison. As shown in the figure, the CHFs expected by the correlation based on the HI exist in a very narrow range of low subcooling near the saturated condition, and they gradually increase with an increase in subcooling. The CHFs are almost independent of pressure for the high subcooling regime. The empirical equation of CHF for subcoolings higher than about 20 K that result from HSN is derived by Eq. (9). The values of K_1, K_2, $q^*_{cr,sat}$ and K_4 are also shown in the table on the figure. The $q^*_{cr,sat}$ results

from the HSN for zero subcooling. The value of $q^*_{cr,sat}$ measured or extrapolated was used for calculations. The measured $q_{cr,sub}$ values for both cylinders lie within ±12% of the values obtained by Eq. (9).

$$q_{cr,sub} = q^*_{cr,sat}(1 + K_4 \Delta T_{sub}^{0.73}),$$
HSN curve for ethanol and FC-72 (9)

As mentioned before, Sakurai et al. [5] have reported that CHF data obtained for high subcoolings at high pressures in a pool of water were due to HSN. In the case of CHF data in a pool of ethanol, which is a highly wetting liquid, it is easy to flood cavities on the cylinder surface. Therefore, it can be seen on the figure that the CHFs from the subcooling near the saturated condition, which are much lower than the CHF of water, are due to HSN. As shown in the regime for the subcoolings higher than about 100 K with the corresponding CHF curves obtained from Eq. (9), the experimental data slightly depends on the pressures, which agrees with the corresponding predicted values. In the case of water, shown in Fig. 4, the CHFs due to HSN derived by Eq. (5) for the high subcoolings at high pressures were almost independent of pressure within the experimental scope. However, it can be assumed that trends of $q_{cr,sub}$ for water similar to those of ethanol will also be obtained when measurements for water are pursued further into higher subcooling ranges. The dependence of pressure on $q_{cr,sub}$ in the high subcooling regime becomes more remarkable in the case of FC-72.

Figure 10 shows the $q_{cr,sub}$ data in FC-72 for the subcoolings ranging from 0 K to 140 K at pressures of 155 kPa, 494 kPa, 886 kPa and 1278 kPa with corresponding HI curves and HSN curves. Concretely, the $q_{cr,sub}$ data at the pressure of 155 kPa are divided into two groups for the subcoolings: the former $q_{cr,sub}$ data agreed with the corresponding HI curve at the saturated condition. The latter $q_{cr,sub}$ for the pressures of 155 kPa to 1278 kPa for the subcoolings are well expressed in the corresponding HSN curves derived from Eq. (9) with the corresponding $q^*_{cr,sat}$ and K_4 values. The values for $q^*_{cr,sat}$ and K_4 were supposed by extrapolation. It should be noted that each HSN curve shown here represents a CHF that results from HSN, and each HSN curve is dependent on pressure. When FC-72 has lower values for properties such as critical pressure or surface tension than those of ethanol, the dependence of pressure on $q_{cr,sub}$ for a high subcooling regime becomes more significant than for ethanol. The transition point in this case is supposed to appear around the saturated condition. This is because the properties of ethanol and FC-72 are very different from each other.

Consequently, the steady-state CHFs show two mechanisms for lower and higher subcooling at various pressures; the former and latter CHFs occur due to HI and HSN, respectively. The dependence of pressure on $q_{cr,sub}$ in the high subcooling regime changed according to the wettability of the boiling liquids involved. It is well known that CHF is considerably affected by properties of boiling liquids that are changeable due to temperature and pressure and other factors. Therefore, the transition phenomena at CHF need further detailed consideration.

3.5 Transient CHF, q_{cr} for Period under Saturated and Subcooling Condition

As shown in the heat transfer process in Fig. 5, the HSN phenomenon could be confirmed on the cylinder surface in pre-pressured water. In addition, the critical heat flux due to HSN in the fully developed nucleation regime caused by a steadily increasing heat input was

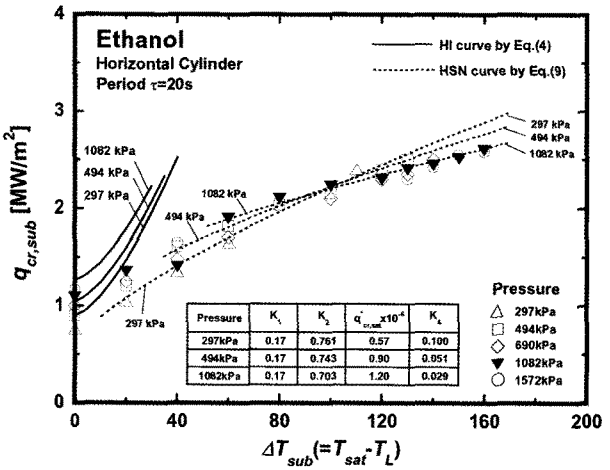

Fig. 9. Comparison of Prediction Representing $q_{cr,sub}$ Related to Subcooling at Pressure as a Parameter in Ethanol using Eqs. (4) and (9)

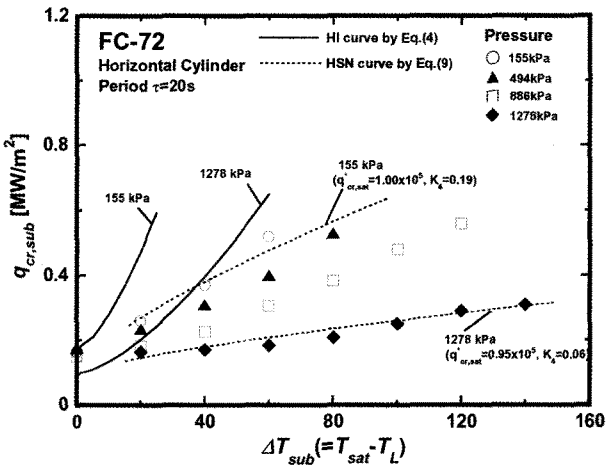

Fig. 10. Comparison of Prediction Representing $q_{cr,sub}$ Related to Subcooling at Pressure as a Parameter in FC-72 using Eqs. (4) and (9)

observed for the first time in a pool of highly subcooled water at high pressure regardless of the pre-pressurization, as shown in Fig. 4. The CHF was significantly lower than the value derived from the CHF correlation obtained based on the HI. It was assumed that the transition to film boiling at the steady-state CHF, $q_{st,sub}$, due to the heat generation rate with a long period such as 20 s for subcoolings higher than around 60 K at pressures higher than around 400 kPa occurs due to the HSN at a lower limit of HSN temperature. Therefore, the trend of q_{cr} values for the periods expressed by Eq. (7), as shown in Fig. 11, become different from the corresponding curve estimated by Eq. (6). Because the steady-state CHF mechanism for highly subcooled water at high pressure was replaced by the HSN from the HI. The q_{cr} data versus the period, τ, also gradually increases with a decrease in period because the HSN surface superheat depends on an increasing rate of surface superheat, as mentioned previously by Sakurai et al [5].

On the other hand, Figs. 12 and 13 respectively show transient CHFs, q_{cr} versus the periods, τ, for different kinds of pressure and subcooling in ethanol and FC-72. As shown in the figures, the q_{cr} values gradually increase with a decrease in period up to the maximum CHF from the steady state CHF that corresponds to the CHF for a period of 20 s or more, then the q_{cr} values suddenly decrease to the minimum value before again increasing as the exponential period decreases. q_{cr} values are classified into three groups according to period τ. It was found that the direct transitions belonging to the second group q_{cr} occur with remarkable frequency. The q_{cr} values belonging to the first group for the ethanol are very dependent on pressure and subcooling, similarly to water. The increasing trend of q_{cr} is explained by the time lag of the heat transfer crisis at the steady-state critical heat flux, q_{st}. However, the q_{cr} values belonging to the first group for the saturated FC-72 are almost independent of pressure, and there is no large difference among the q_{cr} values expressed by Eq. (6). That is why the steady-state CHFs under the saturated condition were also almost independent of pressure, as shown in the Fig. 10.

The minimum q_{cr} values within the second group were much lower than the CHF values within the first group. For example, the minimum q_{cr} value under the pressure of 494 kPa for the saturated ethanol is observed at around 0.4 s, and is marked with ▲ in Fig. 12. It should be noted that the value was about 14% of the CHF value within the first group corresponding to the CHF for the period of 20 s. This fact means that conduction heat transfer becomes more predominant than natural convection heat transfer as the period becomes shorter. Therefore, the heat transfer coefficient becomes higher due to heat conduction, so that a direct or semi-direct transition to film boiling occurs in a remarkable fashion at the heat flux point where the conduction heat transfer is higher than the natural convection heat transfer.

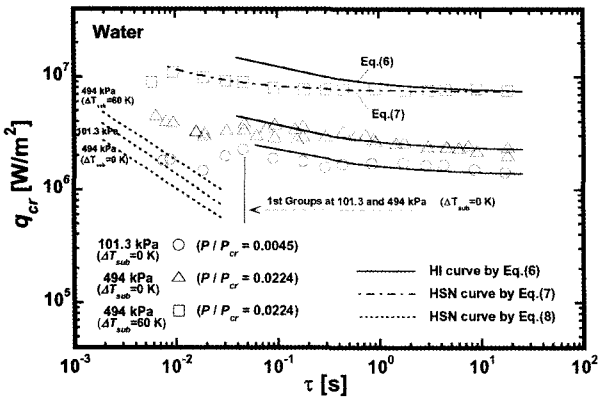

Fig. 11. The Relation between q_{cr} and τ for Different Kinds of Pressure and Subcooling in Water

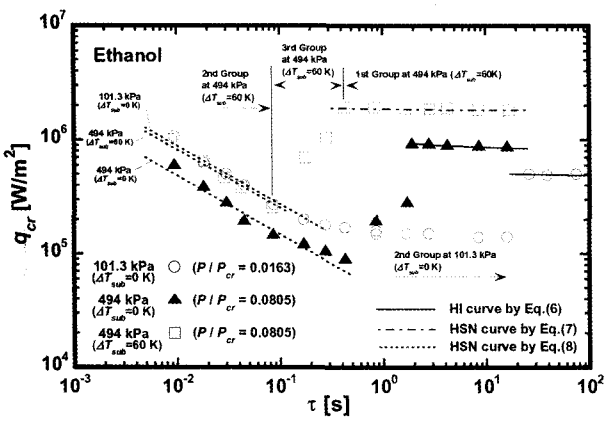

Fig. 12. The Relation between q_{cr} and τ for Different Kinds of Pressure and Subcooling in Ethanol

4. CONCLUSION

This study has investigated the phenomena in the quasi-steady-state or transient boiling CHF that depends on HI and HSN. Major conclusions are as follows:

(1) The steady-state CHFs were divided into two mechanisms for lower and higher subcooling at various pressures; the former and latter CHFs occur due to hydrodynamic instability (HI) and explosive heterogeneous spontaneous nucleation (HSN), respectively.

(2) The dependence of pressure on CHF in the high subcooling regime changed according to the wettability of the boiling liquids involved.

(3) The transient boiling CHFs gradually increased, then decreased quickly and finally increased again as the period became shorter.

(4) The direct transition to film boiling without nucleate boiling was explained by HSN. HSN was particularly likely to occur in transient boiling CHF. The minimum CHFs within the second group were much lower than the CHFs within the first group.

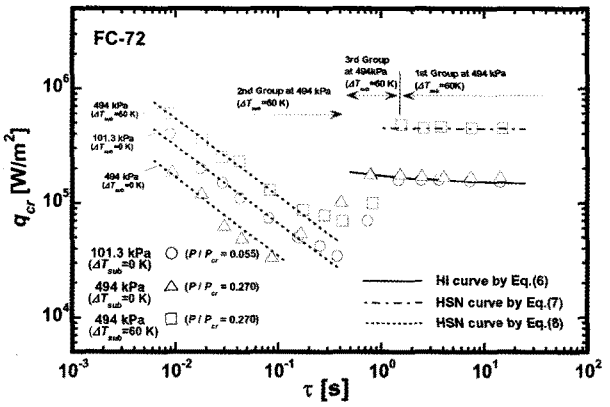

Fig. 13. The Relation between q_{cr} and τ for Different Kinds of Pressure and Subcooling in FC-72

NOMENCLATURE

c_p	specific heat at constant pressure, J/(kgK)
D	cylinder diameter, m
h_c	heat transfer coefficient, W/(m^{2}K)
k	thermal conductivity, W/(mK)
K_1	coefficient in Eq. (4)
K_2	coefficient in Eq. (4)
K_3	coefficient in Eq. (5)
K_4	coefficient in Eq. (9)
L'	non-dimensional length (= $(D/2)\sqrt{g(\rho_l-\rho_v)/\sigma}$)
L_H	Latent Heat of Vaporization, J/kg
P	System Pressure, kPa
P_{cr}	Critical Pressure, kPa
Q	heat generation rate, W/m^3
Q_0	initial heat generation rate, W/m^3
q_{cr}	critical heat flux, W/m^2
$q_{cr,sat}$	q_{cr} for saturated condition, W/m^2
$q^*_{cr,sat}$	q_{cr} due to HSN for zero subcooling, W/m^2
$q_{cr,sub}$	q_{cr} for subcooled condition, W/m^2
q_{st}	steady-state critical heat flux, W/m^2
q_{in}	boiling initiation heat flux, W/m^2
t	time, s
T_w	wall temperature of cylinder, K
T_{sat}	saturation temperature of liquid, K
T_L	bulk liquid temperature, K
ΔT_{in}	boiling initiation superheat, K
ΔT_{sat}	surface superheat (=T_w - T_{sat}), K
ΔT_{sub}	liquid subcooling (=T_{sat} - T_L), K
ρ	density, kg/m^3
g	acceleration of gravity, m/s^2
σ	surface tension, N/m
τ	period, s

subscripts

l	liquid phase
v	vapor phase

REFERENCES

[1] S.S. Kutateladze, "Heat transfer in condensation and boiling", AEC-tr-3770, USAEC (1959).

[2] N. Zuber, "Hydrodynamic Aspects of Boiling Heat Transfer", AECU-4439, USAEC (1959).

[3] S.V. Stralen and R. Cole, "Boiling Phenomena", Vol. 1, *Hemisphere Publ. Co.*, pp. 83-86 (1979).

[4] A. Sakurai, M. Shiotsu & K. Hata, "New transition phenomena to film boiling due to increasing heat inputs on a solid surface in pressurized liquids", *Instability in Two Phase Flow Systems*, **Vol. HTD-260**/Fed-169. ASME, New York, pp. 27-39 (1993).

[5] A. Sakurai, M. Shiotsu and K. Fukuda, "Pool boiling critical heat flux on a horizontal cylinder in subcooled water for wide ranges of subcooling and pressure and its mechanism", *Proceedings of the Thirty-first National Heat Transfer Conference*, **Vol. HTD-326**, ASME, New York, pp. 93-104 (1996).

[6] A. Sakurai, "Mechanisms of transitions to film boiling at CHFs in subcooled and pressurized liquids due to steady and increasing heat inputs", *Nuclear Engineering and Design*, **Vol. 197**, pp. 301-356 (2000).

[7] B.P. Avksentyuk, N.N. Mamontova, "Characteristics of heat transfer crisis during boiling of alkali metals and organic fluids under free convection conditions at reduced pressure", *Prog. Heat Mass Transfer*, **Vol. 7**, pp. 355-362 (1973).

[8] S.S. Kutateladze, V.N. Moskevicheva, G.I. Bobrovich, N.N. Mamontova, B.P. Avksentyuk, "Some peculiarities of heat transfer crisis in alkali metals boiling under free convection", *Int. J. Heat Mass Transfer*, **Vol. 16**, pp. 705-713 (1973).

[9] J. Park, K. Fukuda and Q.S. Liu, "Pool Boiling Critical Heat Flux of Highly Wetting Liquid", The Sixth KSME-JSME Thermal and Fluids Engineering Conference, Jeju, Korea, tfec6-448 (2005).

[10] J. Park, K. Fukuda and Q. Liu, "Pool Boling Critical Heat Fluxes due to Increasing Heat Input in Various Liquids", 17th International Symposium on Transport Phenomena (ISTP-17), Toyama, Japan, pp. 1-8 (2006).

[11] Sutopo P. Fitri, K. Fukuda, Q. Liu, J. Park, "Transient Pool Boiling Critical Heat Flux of FC-72 Under Saturated Conditions", *Journal of Power and Energy Systems*, **1**, 2, pp. 178-189 (2007).

[12] J. H. Lienhard, "Burnout on cylinders", *ASME J. Heat Transfer*, **Vol. 110**, pp.1271-1286 (1988).

[13] K. Fukuda, M. Shiotsu & A. Sakurai, "Transient pool boiling heat transfer due to increasing heat inputs in subcooled water at high pressures", *Proceedings of the 7th International Meeting on Nuclear Reactor Thermal Hydraulics*, Saratoga Springs, USA, pp. 554-573 (1995).

[14] K. Fukuda and A. Sakurai, "Effects of diameters and surface conditions of horizontal test cylinders on subcooled pool boiling CHFs with two mechanisms depending on subcooling and pressure", Heat Transfer 2002, *Proc. of 12th International Conference*, pp. 611-616 (2002).

[15] Y. Takeuchi, K. Hata, M. Shiotsu and A. Sakurai, "A general correlation for laminar natural convection heat transfer from single horizontal cylinders in liquids and gases with all possible Prandtl numbers", International Mechanical Engineering Congress and Exposition, Vol. HTD-317-1. ASME, New York, pp. 259-270 (1995).